

LASER RANGING CORRECTION UNDER MIXED PIXELS EFFECT

Chia-Mien Chang (1), Jen-Jer Jaw (1)

¹ Department of Civil Engineering, National Taiwan University
 No. 1, Sec. 4, Roosevelt Rd., Taipei 10617, Taiwan
 Email: chiamien.chang@gmail.com; jejaw@ntu.edu.tw

KEY WORDS: Correction equation, Functional model, Incidence angle, Pulsed time-of-flight laser ranging, Stochastic model

ABSTRACT: Acquiring high-quality range data of a target lying on discontinuous surfaces by laser range measurement, part of a laser footprint hits accurately at the target feature, while the other part of it casts on the surrounding area, causing mixed pixels effect. Mixed pixels effect can be characterized by multiple ranges within one footprint, thereby leading to erroneous range measurement through a returning deformed waveform. Laser parameters and signal processing approaches vary in rangefinders. Therefore, correction of systematic errors on range data caused by mixed pixels effect will not be the same if employing different instruments. Moreover, without any waveform information, laser ranging correction under mixed pixels effect is difficult, if not impossible, to be treated for most users. This study develops a workflow tackling mixed pixels effect. At first, the parameters in a correction curve are hypothesized from physical property, and then through an experiment, the divergence angle of a laser ranging instrument can be approximated. It follows by an adjustment technique to estimate the correction based on both the functional model formulated by the correction equation and the stochastic model giving appropriate observation quality. For now, considering range distortion caused by mixed pixels effect and incidence angle effect, this study applied the proposed workflow to two different total stations based on time-of-flight laser ranging technique. It shows that if the depth between discontinuous surfaces is within the range resolution, the approach effectively resolves the mixed pixels effect and preserves the range measurement quality.

1. INTRODUCTION

A pulsed time-of-flight (ToF) laser ranging technique with centering and horizontalization has gained widespread acceptance as a powerful tool to execute a target range acquisition in high quality. Through pulse timing estimators to detect timing from returning pulses, this technique attains fine ranging data in most cases (Adams, 1993). However, if the target lies on discontinuous surfaces, a transmitted laser beam splitting and falling on targets with depth (Fig. 1(b)), will lead to mixed pixels effect, causing systematic ranging errors (Herbert & Krotkov, 1992). Mixed pixels effect occurs as long as the distance of a split-up footprint (hereinafter referred to as depth) is shorter than the range resolution δ_r (Eq. (1)). Range resolution refers to the shortest distance a ranging instrument can distinguish between two target points, which can be obtained by calculating the speed of light (c) and pulse width (τ) given in instruction manuals (Eq. (1)). As shown in Fig. 2(a), with only one laser pulse return, mixed pixels effect deceives the rangefinder into the footprint just involving one target to respond unreliable ranging data by a distorted laser pulsed wave (Hsiang, 2001). On the other hand, if the range resolution is shorter than the depth, returning pulse wave with multiple crests evidences individual timing for the rangefinder to compute the corresponding ranging data (Typiak, 2008; Fig. 2(b)).

$$\delta_r = \frac{c \times \tau}{2} \quad (1)$$

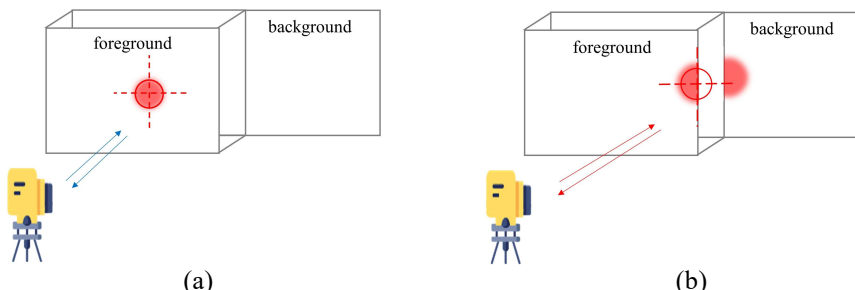


Figure 1. Illustrations of mixed pixels effect (revised from Wang et al., 2016): (a) without mixed pixels effect; (b) the footprint is split and causes mixed pixels effect.

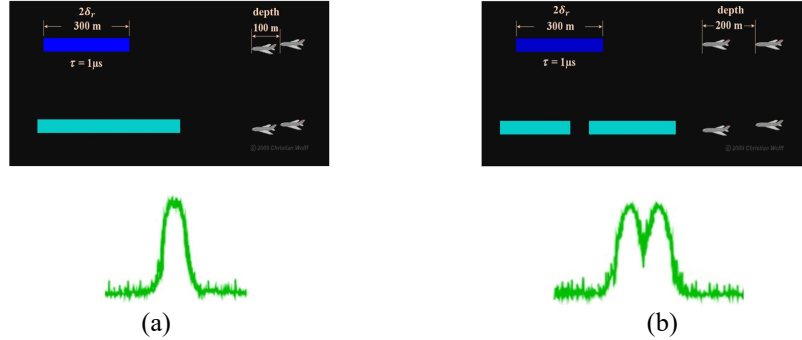


Figure 2. Illustrations of range resolution (revised from Wolff, 2009): (a) the depth is shorter than the range resolution and results in a deformed laser pulse return; (b) the depth is longer than the range resolution and a deformed pulse return with two wave crests is obtained.

Since range measurements are greatly dependent on how they are determined considering several factors, e.g. pulse timing estimators (Fig. 3), transmitted power and divergence angles, it is difficult, if not impossible, to assess the ranging quality in a general form. Even though the ranging errors of a specific instrument can be learnt from waveform analysis and effectively corrected, most of the rangefinders do not reveal waveform information to users (Adams & Probert, 1996), making the ranging errors of mixed pixels effect a stubborn problem. Nevertheless, to restore the ranging quality, other ranging error factors, including incidence angles (Soudarissanane et al., 2009), object distances (Kaasalainen et al., 2011), target reflectances (Okubo et al., 2009), and the shape of targets (Vandapel et al., 2004), combining with mixed pixels need to be well considered.

Analyzing the waveform of a returned pulse in time-intensity (or time-amplitude) observations is crucial to range measurement. As the intensity is converted from the received laser pulse power; therefore, once a received laser power changes, it will also adjust the ranging results. Tan & Cheng (2016) show that the received power P_r is a function of the target reflectances ρ , incidence angles φ , and object distances R by extended Lambertian reflectors (Eq. (2)). Furthermore, the same target point if situated in varied geometry, the received laser power will respond differently and plausibly affect the ranging results (Fig. 4). Thus, to properly correct ranging errors under mixed pixels effect, a consideration of ranging error factors is indeed a must.

$$P_r = C \times \rho \times \cos(\varphi) \times R^{-2} \quad (2)$$

with C a constant parameter about the transmitted power and the divergence angle of a specific ranging instrument.

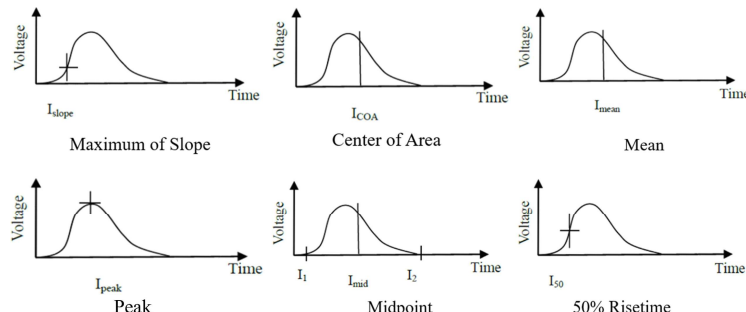


Figure 3. Versatile pulse timing estimators across pulsed ToF laser rangefinders (revised from Abshire et al., 1994).



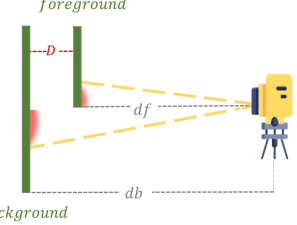
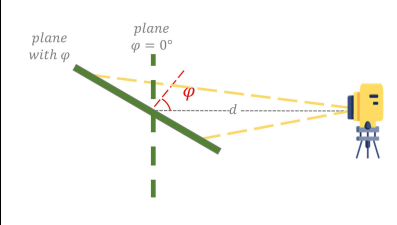
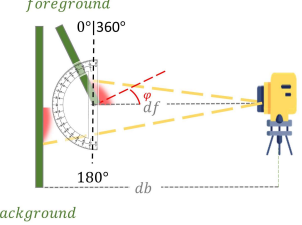
Figure 4. Different target shapes respond to different ranging results.

Yet, as mentioned, it is not common to acquire waveforms when undertaking range measurements. The correction of mixed pixels effect must find its alternative way. This study aims to develop a workflow to fulfill the actual needs of laser ranging correction under mixed pixels effect in the lack of waveform data. The proposed workflow models and derives the parameters of correction equations purely based on range observations, considering ranging error factors and derived parameters to simulate practical ranging arrangement under mixed pixels effect. After collecting those range observations whose depths are within range resolution, it follows by implementing adjustment techniques to fit correction functions with ranging data, and eventually remove or reduce laser ranging errors.

2. LASER RANGING CORRECTION WORKFLOW

To reduce the ranging errors under mixed pixels effect, the primary task is focusing on correcting the ranging errors of case 1 (Tab. 1) where flat foreground and background with the same reflectance are situated apart by a D depth, as the correction of it can effectively suppress significant ranging errors. Moreover, to further restore the ranging quality, introducing influential ranging error factors and applying corresponding corrections would certainly formulate a more rigorous functional model. Case 2 and case 3 are the effort in taking incidence angles into correction model. The developed ranging correction workflow contains initiative realization from physical property, footprint diameter determination, observation collection and arrangements, and adjustment techniques with quality assessment.

Table 1. The conducted cases of ranging correction.

Case 1	Case 2	Case 3
 <p>Mixed pixels effect</p> <p>df: distance to the foreground db: distance to the background D: depth</p>	 <p>Incidence angle effect</p> <p>d: distance to the target φ: incidence angle</p>	 <p>Hybrid of mixed pixels effect and incidence angle effect</p> <p>df: distance to the foreground db: distance to the background φ: incidence angle</p>

2.1 Initiative Realization from Physical Property

Based on Eq. (2), a returning waveform with mixed pixels effect can be approximated shaped, as shown in Fig. 5. The predicted waveform behavior guides establishing the correction model and the parameter estimation accordingly. On the other hand, it also helps learn of how the timing of returning pulse is determined for the employed instrument.

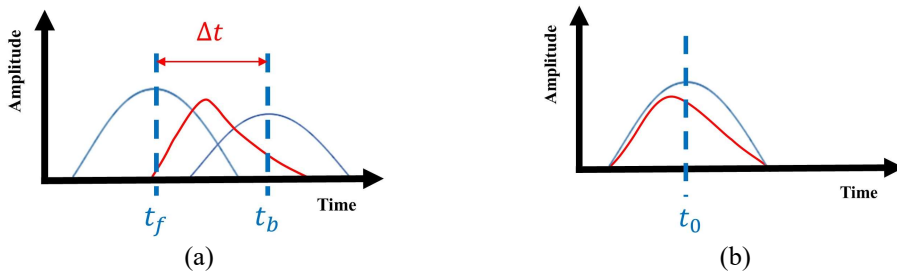


Figure 5. Illustrations of returning waveforms (revised from Hartzell et al., 2013): The blue waves indicate the ideal returning waveform; (a) case 1: the red wave is a distorted waveform of mixed pixels effect; besides, t_f and t_b represent respectively the timing for the foreground measurement and the background measurement; (b) case 2: the red wave is a distorted waveform of incidence angle effect, and t_0 represents the timing of zero incidence angle.

2.1.1 Case 1 (Mixed Pixels Effect): Fig. 5(a) simulates the returning pulse waves of case 1 based on the received laser power-object distance relationship (Eq. (2)). The amplitude of the foreground laser power is larger than that of the background, shifting the wave crest of mixed pixels effect a little bit to the left. Thus, the returning pulse wave deformed by mixed pixels effect will approximately be the red one with the timing error within Δt (Fig. 5(a)) regardless of which timing estimator is used. Based on the pulsed time-of-flight laser ranging equation (Eq. (3)), Δt can be calculated to depth; therefore, the ranging errors of mixed pixels effect can be considered as a function of depths. Besides, by the left-shifted peak of the red wave, one can further anticipate that the responding ranging errors will be slightly smaller than half of the depths.

$$\text{Laser range} = \frac{\text{speed of light}}{2} \times \text{timing} \quad (3)$$

2.1.2 Case 2 (Incidence Angle Effect): An incidence angle is a parameter factor estimated in case 2 correction equation, as received laser power is directly proportional to the cosine of an incidence angle (Eq. (2)). Moreover, incidence angle effect causes a footprint containing multi-range information and part of the footprint closer to the

rangefinder returns stronger intensity (Fig. 6), leading the wave crest to shift slightly to the left (Fig. 5(b)). However, without knowledge about the timing estimator of the instrument, it is still unable to clarify whether the ranging value gets longer or shorter. According to Fig. 5, as the incidence angle grows, the range measurement will increase if the timing is estimated by the peak, while the range measurement decreases if the timing is measured by the midpoint.

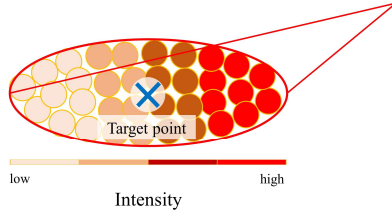


Figure 6. Incidence angle effect incurs the footprint with various return intensities; the farther away from the rangefinder, the lower the intensity.

2.2 Footprint Diameter Determination

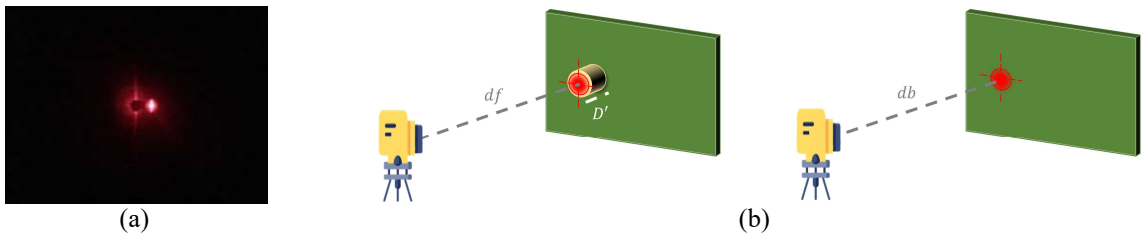


Figure 7. (a) The red area is the guidance of the laser beam, which is not the same as the footprint size of the applied instrument; (b) Illustrations of the proposed experiment to acquire the footprint diameter and the divergence angle of a specific instrument.

To ensure collected ranging data not being distorted by mixed pixels effect, the dimension of laser footprint of applied instruments must be known. As shown in Fig. 7(a), the red area of the laser beam is not necessarily the same as the footprint size; therefore, footprint size information should refer to an instruction manual or to be estimated following the proposed approach. With strict control of the ranging error factors, i.e. the ranging direction of instrument is perpendicular to the target planes, the object distance is fixed, and target planes are with the same reflectance, the ranging errors, as shown in Eq. (4), can be calculated by changing the size of the foreground and collecting actual distances and measured distances:

$$\text{Ranging error (RE)} = df - (db - D') \quad (4)$$

Fig. 7(b) depicts that db is the range of the background measured by a rangefinder, and D' is the depth measured by an instrument with higher ranging quality, so the $db - D'$ can be seen as the actual distance from the instrument to the foreground. df is the range of target foreground measured by the rangefinder, which might cover the ranging errors caused by mixed pixels effect; therefore, it represents the measured distance. By evaluating the difference between the ranging error (Eq. (4)) and the precision of the instrument, it is applicable to check whether the measured results are affected by mixed pixels effect, and further learn of the relationship between the size of the footprint and the current foreground. Thus, after repeating such experiments with enough redundant observations, not only the footprint size can be approximated, the divergence angle of applied instrument can also be determined based on Eq. (5) (Baltsavias, 1999):

$$\text{Divergence angle } (\theta) = \frac{\text{footprint diameter}}{\text{range measurement}} \quad (5)$$

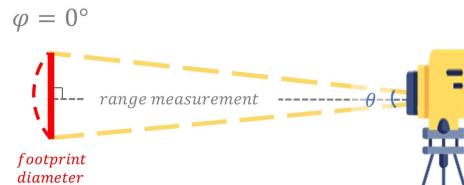


Figure 8. An illustration of deriving divergence angle.

Fig. 8 shows that divergence angles are generally small, so the footprint curve can be approximated as a straight line. Considering both the ranging data and the corresponding footprint diameter are obtained with rigorous arrangements,

a divergence angle can be confidently calculated by carrying out the proposed experiment.

2.3 Observation Collection and Arrangements

Scene arrangements should be based on the physical property (Section 2.1) to prevent the stochastic model from being distorted by the uncertainty of the placement. In addition, to apply observations to subsequent fitting correction equations, at least 30 redundant observations are required to meet the criteria of the statistical standard. In order to ensure the quality of the stochastic model, the target foreground and the background should be nearly parallel to each other and also perpendicular to the applied laser ranging instrument. Here we apply an acrylic sheet combined with a plane table and spirit levels as the target foreground, and a blackboard as the background to fulfill the arrangement setting of case 1. Plus, for eliminating the ranging error factor of target reflectance, both the blackboard and the acrylic sheet are affixed with cardboard to have the same texture and color (Fig. 9(a)).

2.3.1 Case 1 (Mixed Pixels Effect): As revealed in Section 2.1.1, depth is a parameter in ranging error function of mixed pixels effect. Therefore, the correction equation can be fitted by collecting the observations of ranging errors RE (Eq. (6); Fig. 9(b); Fig. 9(c)) and corresponding depths D (Eq. (7)):

$$RE = de - df \quad (6)$$

$$D = db - df \quad (7)$$

where depth D can be calculated by db , a background distance measurement, and df , a distance measurement of the foreground center; while the ranging error RE is composed of the difference between df and the ranging data of targeting at the foreground edge de .

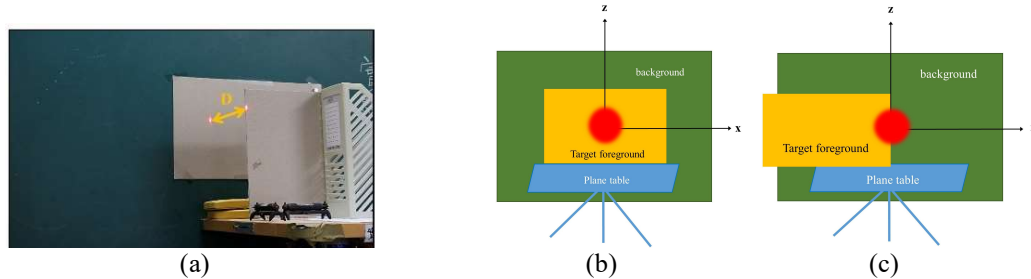


Figure 9. (a) Scene layout of case 1; (b) Ranging acquisition of df ; (c) Ranging acquisition of de .

2.3.2 Case 2 (Incidence Angle Effect): According to section 2.1.2, to fit the ranging correction equations of incidence angle effect, the relationship between the ranging errors RE (Eq. (8)) and the incidence angles must be known. Therefore, apart from general arrangements to collect the ranging results, a protractor is also used to collect the incidence angle observations (Fig. 10).

$$RE = d_{i^\circ} - d_{0^\circ} \quad (8)$$

with d_{i° the ranging data of i incidence angle, and d_{0° the ranging data of zero incidence angle.

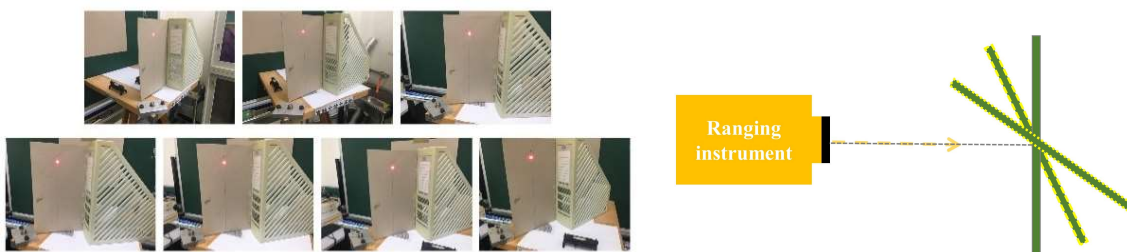


Figure 10. Illustrations of scene layout in case 2.

2.4 Adjustment Techniques with Quality Assessment

Using scatterplots to visualize the collected observations and analyze the relationship and trends between observations to determine an appropriate functional model. After that, the collected data is treated with generalized least-squares

adjustment to solve the parameters of the ranging correction equation. Furthermore, to ensure the quality of the correction equation, the fitting results need to be checked by the following theoretical precision indicators (Kermarrec et al., 2018). A posteriori variance factor evaluates the overall model quality by checking the ratio of a posteriori variance factor to a priori variance factor. If the ratio is close to 1, it indicates that the overall model is reasonable. A residual vector shows the distribution of observations to a fitted curve. And observations with large outliers can be removed to refine the fitting curve. Quality of model parameters is a quality index to assess the least-square adjustment. By comparing the uncertainties of the parameters with the instrument random errors to clarify whether the least-squares results meet the quality requirements. Furthermore, to optimize the functional model, tests of significance should be conducted to acquire a rigorous mixed pixels effect correction equation neither under- nor over-fitting.

The indicators, including a posteriori variance factor, a residual vector, and quality of model parameters, can only confirm the internal precision of the correction equation; therefore, external accuracy evaluation should be performed by reliable checkpoints to clarify whether the adjustment results are performed with sufficient quality. Root mean square error (RMSE) is employed to assess the true (or nearly true) error of the proposed model upon correction and helps reveal the systematic error, if existing, and thus remodel the correction function to refine the results, while root mean square difference (RMSD) is considered if the checkpoints are with certain amount of errors.

3. EXPERIMENT RESULTS AND ANALYSIS

To evaluate whether the quality of the proposed workflow meets practical requirements, experiments of case 1, case 2, and case 3 are conducted, and the results are presented in this section. Besides, to further clarify the performance of the laser ranging correction workflow under mixed pixels effect, two total stations, as specified in Tab. 2, equipped with pulse time-of-flight laser ranging technology are utilized in case 1 and case 2 to collect data.

Table 2. The specifications of employed equipment.

	Illustration	Distance precision from manufactures	Distance precision estimated from experiments	Divergence angle estimated from experiments
Trimble M3 DR2"		±10mm	±0.5mm	0.1326°
Topcon GPT-3002LN		±10mm	±1.5mm	0.1217°

3.1 Footprint Diameter Determination

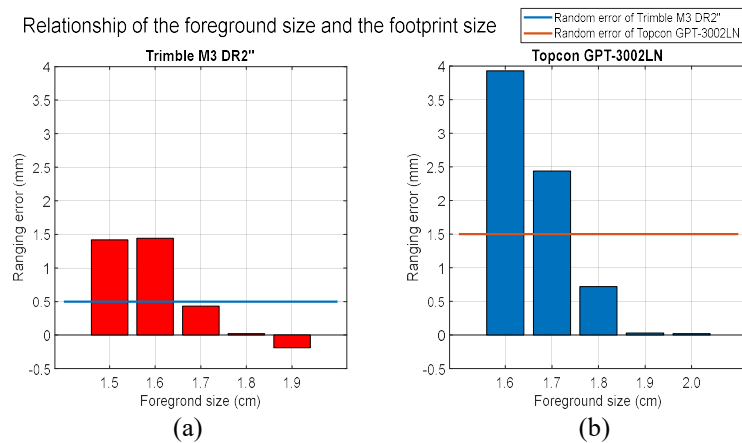


Figure 11. Data collection results to determine the footprint diameters: (a) Trimble M3 DR 2" with the object distance 6.916m; (b) Topcon GPT-3002LN with the object distance 8.238m.

The data for estimating divergence angles can be collected by carrying out the procedure stated in section 2.2. According to Fig. 11(a), when the foreground size is 1.6cm, the ranging error is apparently larger than the random

error of Trimble M3 DR 2"; while the foreground size scales up to 1.7cm, the ranging error is going below it, indicating that the footprint size is between 1.6cm to 1.7cm as the object distance is 6.916m. Bringing the data into Eq. (5), 0.1326° turns out to be the divergence angle of Trimble M3 DR 2". Similarly, the divergence angle of Topcon GPT-3002LN is found as 0.1217° .

3.2 Case 1 (Mixed Pixels Effect)

Tab. 3 and Tab. 4 show that the mixed pixels effect ranging bias is approximately half of the corresponding depth, which matches the results of physical property (Section 2.1.1). Thus, through fitting the collected data to a linear function (Tab. 3(a); Tab. 4(a)), the mixed pixels effect laser ranging correction equations are modeled and put into adjustment. Moreover, collecting depth data by a vernier caliper with $\pm 0.03\text{mm}$ ranging precision as true value, the computed RMSE of both the instruments are found to be all within their random errors (Tab. 2). It indicates that the decimeter-level ranging errors of the mixed pixels effect can be significantly reduced by the correction equations, and also the effectiveness of the correction workflow under mixed pixels effect for pulsed time-of-flight laser ranging techniques is proved to be valid.

Table 3. Ranging correction results of mixed pixels effect: Trimble M3 DR2".

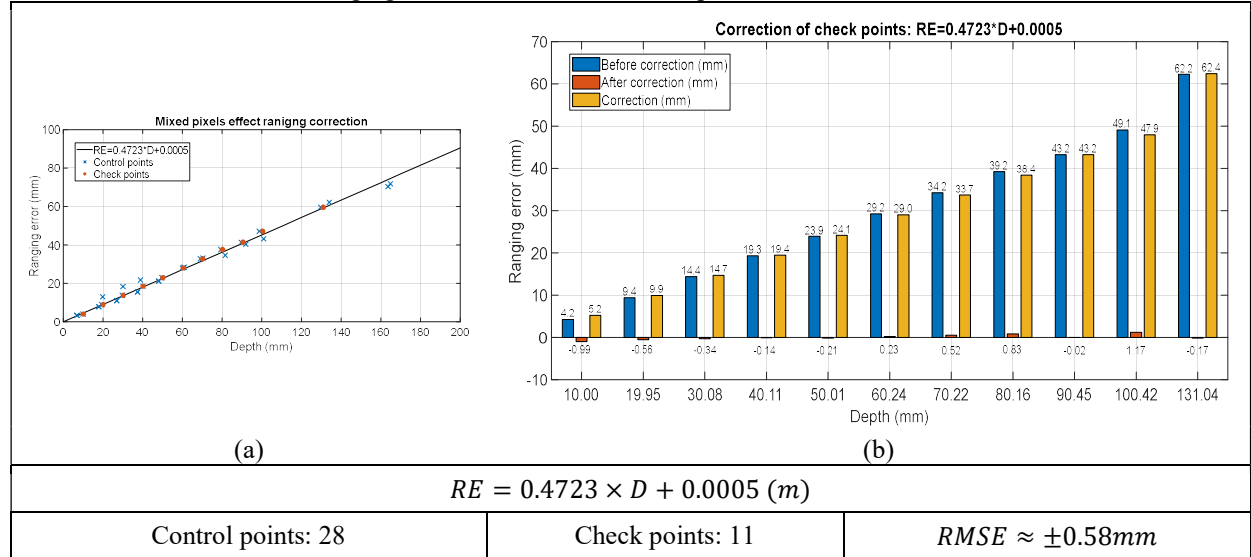
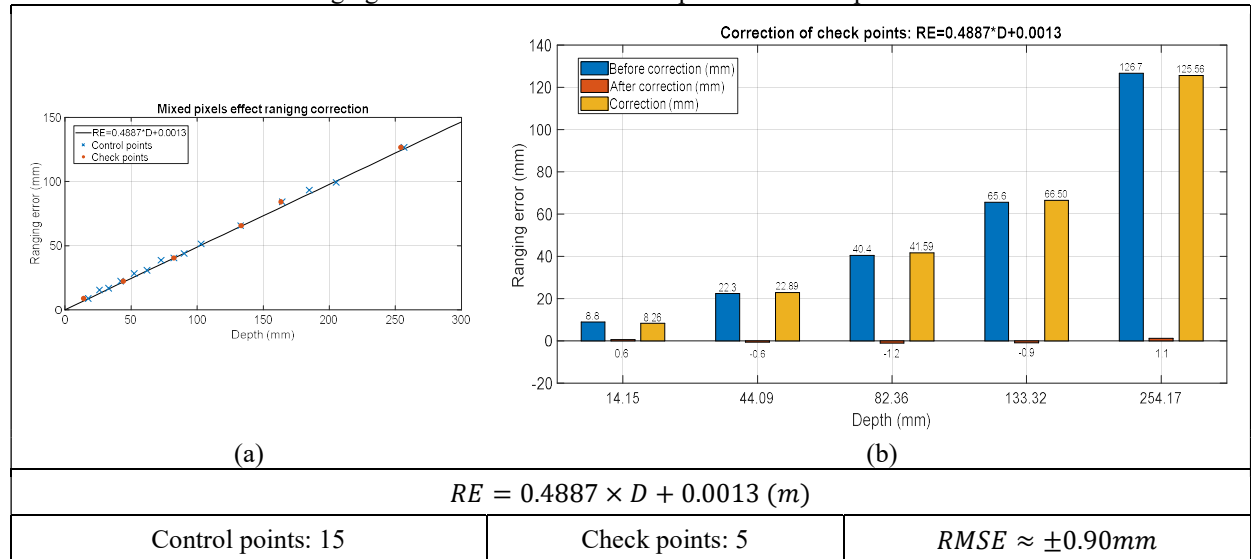


Table 4. Ranging correction results of mixed pixels effect: Topcon GPT-3002LN.



3.3 Case 2 (Incidence Angle Effect)

According to Fig. 5(b), it is anticipated that the incidence angle effect may not be noticeable as case 1 and how the timing estimator is employed in individual instrument would strongly affect the error behavior. Case 2 experiments

test two total stations, and find that ranging data of Trimble M3 DR2" is gradually decreasing with the incidence angle increasing, while Topcon GPT-3002LN performs in the other way (Fig. 12). It verifies that the two instruments use different timing estimators and affect the ranging errors with different signs.

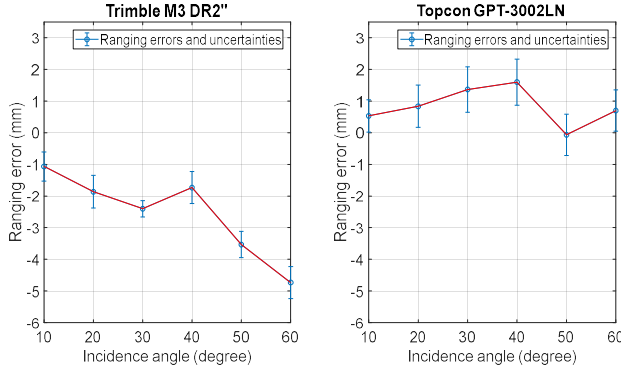
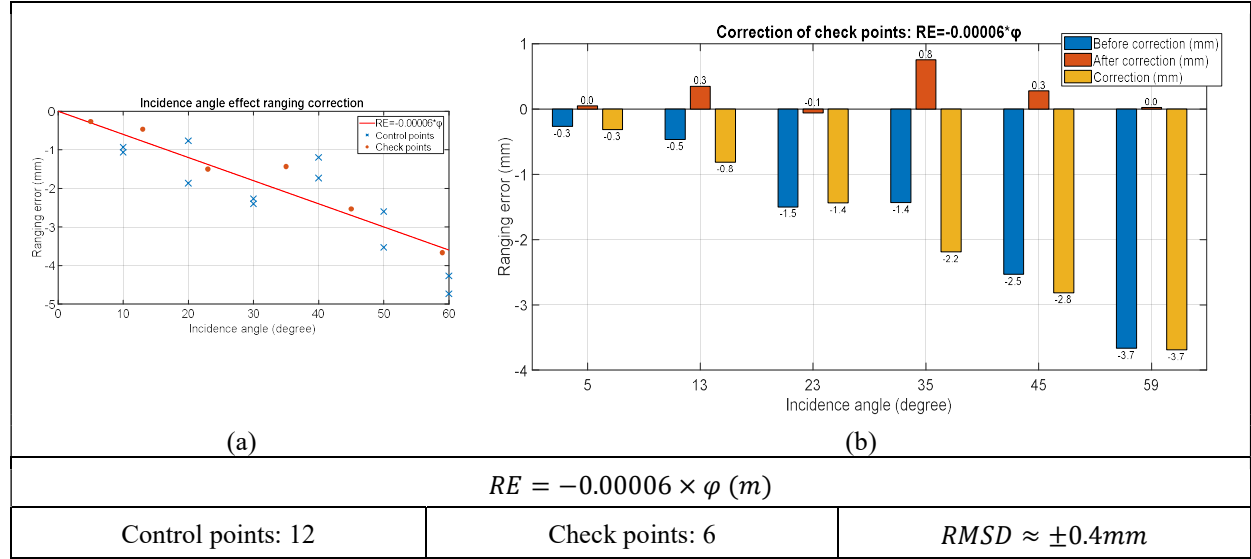


Figure 12. Ranging errors of incidence angle effect by different instruments.

To estimate the ranging errors of incidence angle effect, enough range observations are needed to deploy the fitting model. Tab. 5 (a) shows that the overall ranging errors caused from 0° to 60° incidence angles are approximately $\pm 2.7\text{mm}$, which are actually smaller than the precision $\pm 10\text{mm}$ provided by the manufacturers (Tab. 2). Namely, without particular tackling the incidence angle effect, the ranging results will cover about 3mm ranging errors. Nonetheless, following the proposed workflow, the RMSD drops to $\pm 0.4\text{mm}$, reporting that the workflow can still refine the ranging results of Trimble M3 DR2" by reducing the ranging errors from mm-level to under mm-level (Tab. 5 (b)).

Table 5. Ranging correction results of incidence angle effect: Trimble M3 DR2".



3.4 Case 3 (Hybrid of Mixed Pixels Effect and Incidence Angle Effect)

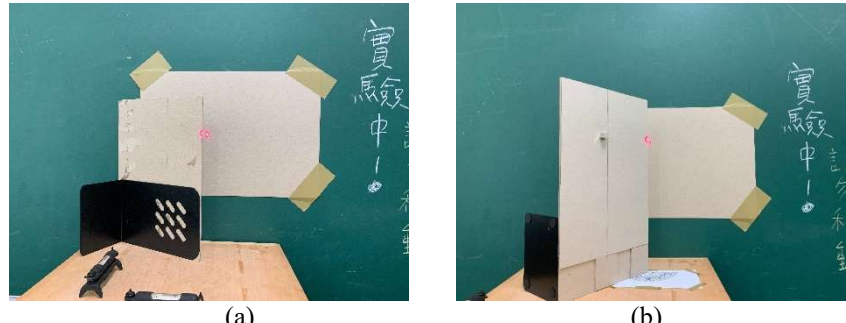


Figure 13. The experiment scene of with both mixed pixels effect and incidence angle effect.

Intuitively, through joining the correction equations of mixed pixels effect and incidence angle effect, the ranging errors in case 3 should be corrected. However, various configurations, Fig. 10 (case 2), Fig. 13(a) (case 3), and Fig. 13(b) (case 3) for example, of incidence angles may result in different ranging errors.

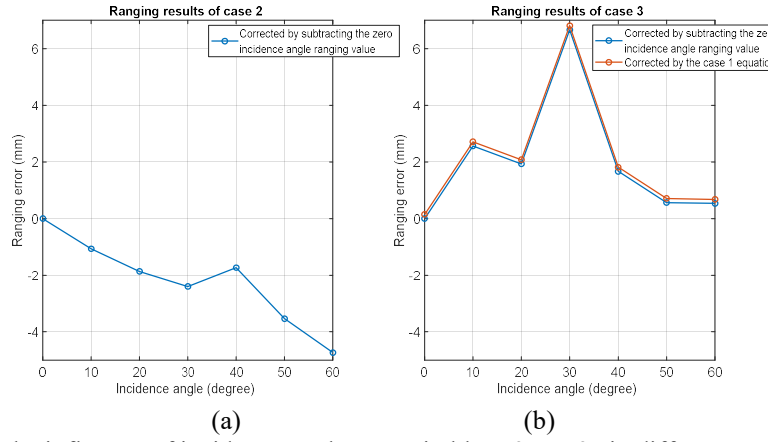


Figure 14. Comparing the influence of incidence angles on Trimble M3 DR 2'' in different cases: (a) case 2 (Fig. 10); (b) case 3 (Fig. 13(a)).

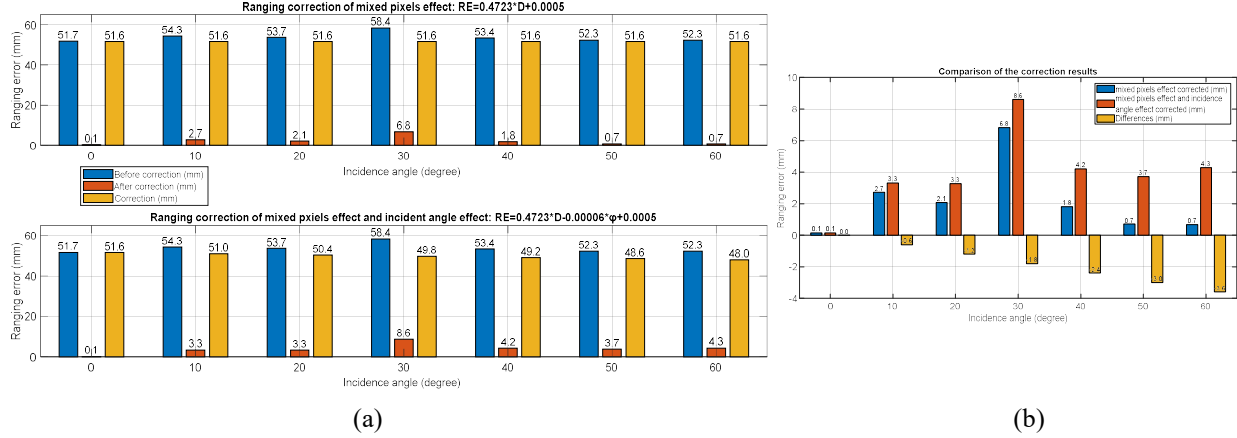


Figure 15. The results of implementing different correction equations to case 3 (Fig. 13(a)).

Two results of incidence angle effect in case 3 (Fig. 13(a)) are estimated by removing the mixed pixels effect, as shown in Fig 14(b). The one with the subtraction of mixed pixels effect using case 1 model from the measured range is in a high agreement with that obtained by the difference of range measurements all referred to zero incidence angle. Even though the collected data of case 3 (Fig. 13(a)) contains an outlier, i.e. ranging results of 30° incidence angle (Fig. 14(b)), its ranging errors perform quite differently from case 2 (Fig. 14(a)). Upper part of Fig. 15(a) reveals that the overall ranging error of case 3 after correcting mixed pixels effect is $\pm 1.6\text{mm}$, which already meets the ranging precision provided by the manufacturer (Tab. 2). However, if simply adding up the models of case 1 and case 2, the ranging results might get worse after correction (lower part of Fig. 15(a)), highlighting that the hybrid of mixed pixels effect and incidence angle effect cannot be simply modeled as the addition of case 1 and case 2 and needs to be further considered based on the errors estimated, as shown in Fig. 14(b). Moreover, Fig. 14(b) also reveals that by bringing the correction equation of the mixed pixels effect (case 1) into the hybrid case, the ranging errors are quite similar to the results subtracting zero incidence angle ranging data from the ranging results. It shows how effective the correction equation is in tackling the ranging errors of mixed pixels effect.

4. CONCLUSION AND FUTURE WORK

4.1 Conclusion

This study presents a laser ranging correction workflow, aiming to correct ranging errors under mixed pixels effect without any physical waveform information. At this stage, two total stations with pulsed ToF laser ranging technology are conducted to examine the effectiveness of the developed workflow. Comparing the RMSEs with the random errors of the applied instruments, it shows that the laser ranging errors of the mixed pixels effect can be effectively removed by the proposed workflow. Plus, to refine the correction equation under mixed pixels effect, incidence angle

effect is introduced. According to the experiment results of case 2, the mm-level ranging errors caused by the incidence angle effect are within the precision provided by the manufactures, and they can be further corrected by the presented workflow to reach up under mm-level. Though the correction of the incidence angle effect in case 3 still has room to improve, the mixed pixels effect is significantly removed by the correction equation of case 1, indicating mixed pixels effect is stable and can be well controlled.

4.2 Future Work

For achieving a better correction result, it deserves to pay more attention to formulate an appropriate model in diminishing or reducing the remaining ranging errors when faced with both mixed pixel effect and incidence angle effect. Moreover, other ranging error factors, i.e. object distances, target reflectances, and the shape of targets, should be introduced to well clarify their roles in modeling correction equations, thus removing or reducing the laser ranging errors under mixed pixels effect to the most optimization.

5. REFERENCE

- Abshire, J. B., J. F. McGarry, L. K. Pacini, J. B. Blair, & G. C. Elman, 1994. Laser altimetry simulator. Version 3.0: User's guide.
- Adams, M. D., 1993. Amplitude modulated optical range data analysis in mobile robotics, In: IEEE International Conference on Robotics and Automation, pp. 8-13.
- Adams, M. D., & P. J. Probert, 1996. The interpretation of phase and intensity data from AMCW light detection sensors for reliable ranging. *The International journal of robotics research*, 15 (5), pp. 441-458.
- Baltsavias, E. P., 1999. Airborne laser scanning: basic relations and formulas, *ISPRS Journal of photogrammetry and remote sensing*, 54(2-3), pp. 199-214.
- Hartzell, P. J., C. L. Glennie, & D. C. Finnegan, 2013. Calibration of a terrestrial full waveform laser scanner. American Society for Photogrammetry and Remote Sensing.
- Hsiang, 2001. Radar system. Publishing House of Electronics Industry, pp. 8-15.
- Hebert, M., & E. Krotkov, 1992. 3D measurements from imaging laser radars: how good are they? *Image and vision computing*, 10 (3), pp. 170-178.
- Kaasalainen, S., A. Jaakkola, M. Kaasalainen, A. Krooks, & A. Kukko, 2011. Analysis of incidence angle and distance effects on terrestrial laser scanner intensity: Search for correction methods. *Remote Sensing*, 3 (10), pp. 2207-2221.
- Kermarrec, G., H. Alkhatib, & I. Neumann, 2018. On the Sensitivity of the Parameters of the Intensity-Based Stochastic Model for Terrestrial Laser Scanner. Case Study: B-Spline Approximation. *Sensors*, 18 (9), pp. 2964.
- Okubo, Y., C. Ye, & J. Borenstein, 2009. Characterization of the Hokuyo URG-04LX laser rangefinder for mobile robot obstacle negotiation. *Unmanned Systems Technology XI*, p. 733212.
- Soudarissanane, S., R. Lindenbergh, M. Menenti, & P. J. G. Teunissen, 2009. Incidence angle influence on the quality of terrestrial laser scanning points. *ISPRS Workshop Laserscanning*, Paris, France, 1-2 Sept 2009.
- Tan, K., & X. Cheng, 2016. Correction of incidence angle and distance effects on TLS intensity data based on reference targets. *Remote Sensing*, 8 (3), pp. 251-270.
- Typiak, A., 2008. Use of laser rangefinder to detecting in surroundings of mobile robot the obstacles. In: Symposium on Automation and Robotics in Construction, pp. 26-29.
- Vandapel, N., O. Amidi, & J. R. Miller, 2004. Toward laser pulse waveform analysis for scene interpretation. In: IEEE International Conference on Robotics and Automation, pp. 950-955.
- Wang, Q., H. Sohn, & J. Cheng, 2016. Development of a mixed pixel filter for improved dimension estimation using AMCW laser scanner. *ISPRS Journal of Photogrammetry and Remote Sensing*, 119, pp. 246-258.
- Wolff, C., 2009. Radartutorial.eu, Retrieved July 26, 2019, from <http://www.radartutorial.eu/01.basics/Range%20Resolution.en.html>.